Macromolecular Research, Vol. 24, No. 5, pp 422-428 (2016)
DOI 10.1007/s13233-016-4053-1

www.springer.com/13233
pISSN 1598-5032 eISSN 2092-7673

Ionic Interactions and Dielectric Relaxation of PEO/PVDF-Mg[$(CF_3SO_2)_2N_2$)] Blend Electrolytes for Magnesium Ion Rechargeable Batteries

R. Rathika* and S. Austin Suthanthiraraj

Department of Energy, University of Madras, Guindy Campus, Chennai-600025, India

Received November 19, 2015; Revised February 11, 2016; Accepted February 26, 2016

Abstract: A new series of magnesium-ion conducting solid polymer blend electrolytes based on an optimized blend ratio (90:10) of poly(ethylene oxide) (PEO) and poly(vinylidene fluoride) (PVDF) doped with different concentrations of magnesium bis (trifluoromethane sulfonimide) salt, Mg [$(CF_3SO_2)_2N_2$)] has been prepared by solution casting technique, using dimethylformamide (DMF) as the common solvent. The increase in the amorphous phase with an increase in salt concentration of the prepared blended polymer electrolytes has also been nurtured from the results obtained from X-ray diffraction (XRD) and scanning electron microscopic (SEM) analyses. The electrical transport characteristics were evaluated by means of electrochemical impedance spectroscopy (EIS) and the maximum ionic conductivity obtained at room temperature (298 K) was found to be 1.2×10^{-5} S cm^{-1} in the case of the blend containing 15 wt% salt. A detailed investigation concerning the mechanism of magnesium ion transport in the optimized polymer blend electrolyte over the frequency range of 1 MHz to 20 Hz has also been carried out in terms of electrical conductivity spectra, dielectric properties and electrical modulus spectra at room temperature.

Keywords: poly(ethylene oxide)/poly(vinylidene fluoride), blend polymer electrolytes, AC-impedance, X-ray diffraction, Scanning electron microscopy, dielectric behaviour.

Introduction

The rapid development of polymer electrolytes has drawn the attention of many researchers in the last three decades as they find applications not only in secondary batteries but also in other electrochemical devices such as supercapacitors, electrochromic displays, sensors, smart windows, fuel cells, and so on.[1,2] Moreover, the global interest on modern energy technology, especially energy storage technology currently reveals more attention in electronic miniaturization with desired shapes. However, the family of polymer electrolytes with sufficient ion transport is playing a crucial role towards the development of high-performance energy storage devices due to their versatility, safety and easy handling over the conventional organic liquid electrolytes.[3-7] Poly(ethylene oxide), PEO based solid polymer electrolyte have been attractive as one of the most promising candidates because of its solvating ability with adequate ionic conductivity at room temperature.[8] In addition to that, the semi-crystalline nature of PEO limits the ion transport at ambient temperature. The amorphous nature is a primary concern to achieve sufficient ionic conductivity which can be obtained by modifying the electrolyte matrix with addition of plasticizers, by the addition of ceramic fillers, or by modification of polymer like blending.[8-11] There have been numerous attempts to reduce the crystallinity of PEO; the introduction of polymer blending is one of the most successful ways to overcome the drawback. Interestingly, poly(vinylidene fluoride), PVDF characterized with a low ionic range and high electro-negativity interacts with electron donor groups of PEO to create the PEO-PVDF polymer blends. Such blends decrease the crystallinity of PEO thus improving the degree of dissociation of salt, chain mobility (especially at room temperature), and increases the dimensional stability even at high temperatures as well.[12-15]

The current lithium-ion battery technologies are facing severe challenges with regard to the safety, cost and environmental aspects as well as the concern arising on the scarcity of lithium resources in the Earth's crust. However, despite the fact that most of the R&D are concentrated on lithium-ion batteries, a viable alternative is in urgent need.[16-19] Research on non-lithium energy storage systems have now re-emerged world-wide.[20-24] In accordance with the above mentioned important aspects of this research, Mg is included on several reports in association with lithium in terms of safety and cost despite having difficulties in choosing the potential electrolyte to match the narrow electrochemical potential window.[25,26] It is quite obvious from the literature that the use of organic liquids with magnesium salt is no longer to be the good idea because of its tendency to form a thin passivation layer on the surface of the magnesium anode. Therefore, much effort has been devoted

*Corresponding Author. E-mail: rathikawin@gmail.com

to develop suitable electrolytes with high anodic stability as well as suitability for magnesium deposition or dissolution.

Here, we present a detailed analysis of magnesium-ion conducting polymer blend solid electrolytes initiating the complex formation between the poly(ethylene oxide) (PEO), poly (vinylidene fluoride) (PVDF), and magnesium bis (trifluoromethane sulfonimide) Mg [$(CF_3SO_2)_2N_2$)] salt by using a solution casting technique. The structural and surface morphology of these polymer blend electrolytes have been thoroughly characterized by using X-ray diffraction and scanning electron microscopy studies. The properties of different concentrations of magnesium salt on ionic conductivities have been measured by using an electrochemical impedance spectroscopy technique. Importantly, detailed analysis of frequency response of electrical conductivity, dielectric properties and electrical modulus spectra has been done at room temperature in order to identify the ion transport mechanism of magnesium ion for all the six different salt concentrations investigated.

Experimental

Starting Materials. Commercially available chemicals of poly(ethylene oxide) PEO (molecular weight (MW)=5×10^6 g/mol), poly(vinylidene fluoride) PVDF (MW=275,000 g/mol) and the salt namely magnesium bis (trifluoromethane sulfonimide) Mg [$(CF_3SO_2)_2N_2$)] (MW=584.60 g/mol) were procured from Sigma-Aldrich and used as- received.

Preparation of the Solid Polymer Electrolytes. A series of solid polymer blend electrolytes containing the formation of PEO-PVDF + x wt% salt (where x=3, 6, 9, 12, 15, and 18) has been prepared by using solution casting technique using dimethylformamaide (DMF) as the common solvent. Initially, the polymer blend was prepared by dissolving 0.45 g of PEO and 0.05 g of PVDF in 35 mL of dimethylformamaide (DMF) under continuous stirring at 353 K. Subsequently different concentration of magnesium salt was added into the above polymer blend at an ambient environment. The mixture was then stirred continuously until the solution becomes a homogenous viscous solution which was then solvent cast onto glass petri dishes and maintained at 60 °C for DMF to evaporate and vacuum dried at 333 K for 15 h to aid solvent evaporation. The resulting thin polymer films were stored in a desiccator to evade the moisture for further analysis.

Analysis. The electrical conductivities of the polymer-blend electrolyte films were determined using AC impedance measurements performed on all the samples using a computer-controlled Hewlett-Packard model HP 4284 Precision LCR meter in the frequency range 1 MHz-20 Hz in the room temperature 25 °C. The solid polymer electrolyte films were presented between two polished stainless steel electrodes (SS) and such symmetrical cells involving blocking interfaces with the configuration - [SS/SPE/SS] were utilized for electrical impedance measurements. The electrical conductivity of the polymer-blend electrolyte (σ) was calculated using the equation:

$$\sigma = \frac{t}{R_b \cdot A} \tag{1}$$

where, t is the thickness of the polymer-blend electrolyte film, R_b the bulk resistance and A is the area of the contact. The value of R_b was evaluated from the observed low frequency intercept of the semicircle on the real axis of the complex impedance plot.

X-Ray diffraction measurements were performed using an X′ pert-pro diffraction system with $CuK_{\alpha1}$ radiation (λ=1.54060 Å) at room temperature in the scanning angle 2θ between 10 to 60°.

The surface morphology of the thin films of solid polymer-blend electrolytes was characterized at room temperature by means of a Vega 3 Tescan and the samples were coated with a slight layer of gold by vacuum sputtering for 20 s in order to prevent electrostatic charging.

Results and Discussion

X-Ray Diffraction Analysis. Figure 1 depicts the set of room temperature X-ray diffraction (XRD) patterns obtained for pure PEO, PEO-PVDF blend and PEO-PVDF blended with six different amounts of the chosen salt, Mg [$(CF_3SO_2)_2N_2$] *viz.*, 3, 6, 9, 12, 15, and 18 wt% respectively. It is quite obvious from Figure 1 that a pair of characteristic XRD peaks appear at scanning angles (2θ) of 19.19 and 23.5°, respectively in the case of the typical XRD pattern obtained for pure PEO material owing to its semi-crystalline nature. On the other hand, blending of PEO with PVDF has been found to result in a considerable decrease in the intensity of the above XRD peaks as evident from the XRD pattern noticed for the PEO - PVDF polymer-blend. In other words, the incorporation of PVDF into the matrix of PEO has effectively reduced the crystallinity of the host polymer namely PEO. However, it is interesting to note from Figure 1 that doping of PEO-PVDF polymer-blend with various amounts of Mg [$(CF_3SO_2)_2N_2$] salt would effectively bring about certain significant changes within the structural framework of the polymer-blend in terms of varying degrees of the crystallinity as suggested by the tendency of XRD patterns corresponding to different amounts of the salt incorporated into the polymer-blend system.

Eventually, Figure 1 shows that when the amount of the dopant salt Mg [$(CF_3SO_2)_2N_2$] within the PEO-PVDF polymer-blend is increased from 3 to 6 wt% the observed intensity of XRD peaks occurring at 2θ=19.19 and 23.5° decreases while further addition towards 9, 12, 15, and 18 wt% has been associated with an increased intensity and sharpening of the XRD peak in general, thereby revealing the feasibility of an apparent enhancement in the degree of crystallinity in the case of salt-rich compositions beyond 9 wt% loading. This implies that the lowest intensity of the diffraction peak occurring at 6 wt% salt concentration is expected to yield an enhanced electrical conductivity of this particular sample when compared to the remaining compositions. However, the fact that

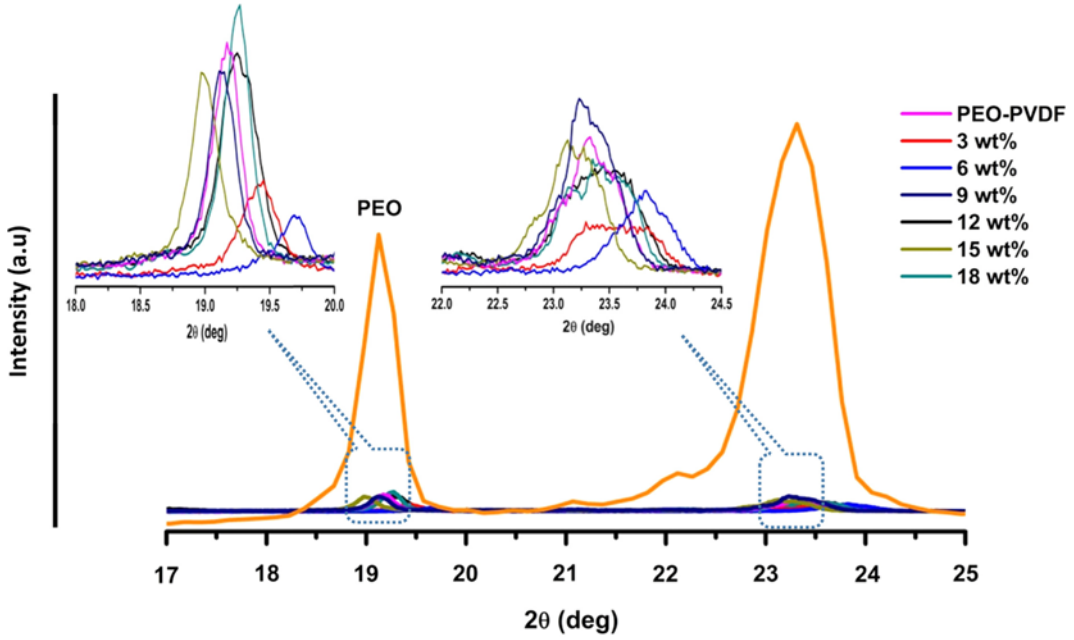

Figure 1. Room temperature X-ray diffraction (XRD) patterns of pure PEO, PEO-PVDF blend and PEO-PVDF blended samples having six different concentrations of the salt.

the typical composition containing 15 wt% salt exhibits the maximum electrical conductivity at room temperature instead of 6 wt% sample may be attributed to the most probable optimized structural and compositional environment provided by the doping of 15 wt% salt into the PEO-PVDF polymer-blend system under the present investigation.

In this context, it is also reasonable to argue that the predominant dilution effect occurring in the case of 3 and 6 wt% salt - added compositions, despite the fact of possessing appreciably low intensity XRD peaks with reduced crystallinity may be responsible for the insufficient number of mobile ions namely Mg^{2+} ions available for the conduction process thereby yielding low values of electrical conductivity in such blended systems. These aspects are found to be in good agreement with relevant electrical conductivity results presented in a subsequent section as well.

Morphological Analysis. The surface morphology of PEO-PVDF polymer blend and that of the blend with varying concentrations of salt incorporated has been observed by scanning electron microscopy (SEM). Figure 2(a) shows the photograph of as-prepared transparent thin film of PEO-PVDF solid blend polymer electrolyte whereas Figure 2(b)-(j) depicts the SEM micrographs of blend polymer, containing six different salt contents *viz*., 3, 6, 9, 12, 15, and 18 wt% and the energy dispersive X-ray spectroscopy (EDAX) pattern of PEO-PVDF and the blend with 15 wt% salt added system respectively. As seen in Figure 2(b), the blend PEO-PVDF still displays a spherulite surface but not rough spherulites with pores, reflecting semi crystalline nature of PEO. The spherulites disappear gradually and become smooth when the salt concentration rose from 3 to 15 wt% Figure 2(c)-(g) and tend to infer the deduction of the crystallinity. The spherulites have completely disappeared at 15 wt% salt content thus revealing that the prepared blend electrolyte becomes more amorphous which is in agreement with XRD data. Beyond this concentration, an incomplete salt dissociation or ion aggregates is observed as evidenced by the presence of Mg particles on the surface of the film at the salt content of 18 wt% (Figure 2(h)).

Electrical Conductivity Analysis. The Nyquist plots (Z' *vs*. Z'') of the impedance data obtained for the freshly prepared polymer blend electrolytes (PEO-PVDF: x wt% salt) with different salt concentrations at room temperature are shown in Figure 3(a) and (b). In general, the low frequency intercept of the semicircle on the real axis of the impedance plot represents the bulk electrolyte resistance (R_b) and is inversely proportional to the ionic conductivity as given in Eq. (1). It is clearly seen from Figure 3(a) and (b) that the observed diameter of the semicircle on the real axis decreases as a function of salt concentration increases from 3 to 15 wt% followed by the intercept of semicircle and increases for the remaining salt concentration (18 wt%). The lowest vale of bulk resistance was observed for the salt concentration of 15 wt% which results in the maximum conductivity of 1.2×10^{-5} S cm^{-1} at room temperature whereas a decrease in conductivity is observed in the case of higher loading of salt concentration as shown in Figure 3(c). As the salt concentration increases the value of conductivity is increased monotonically up to 15 wt% at room temperature (298 K). The increase in the ionic conductivity with the increase of salt concentration may be related to the increase

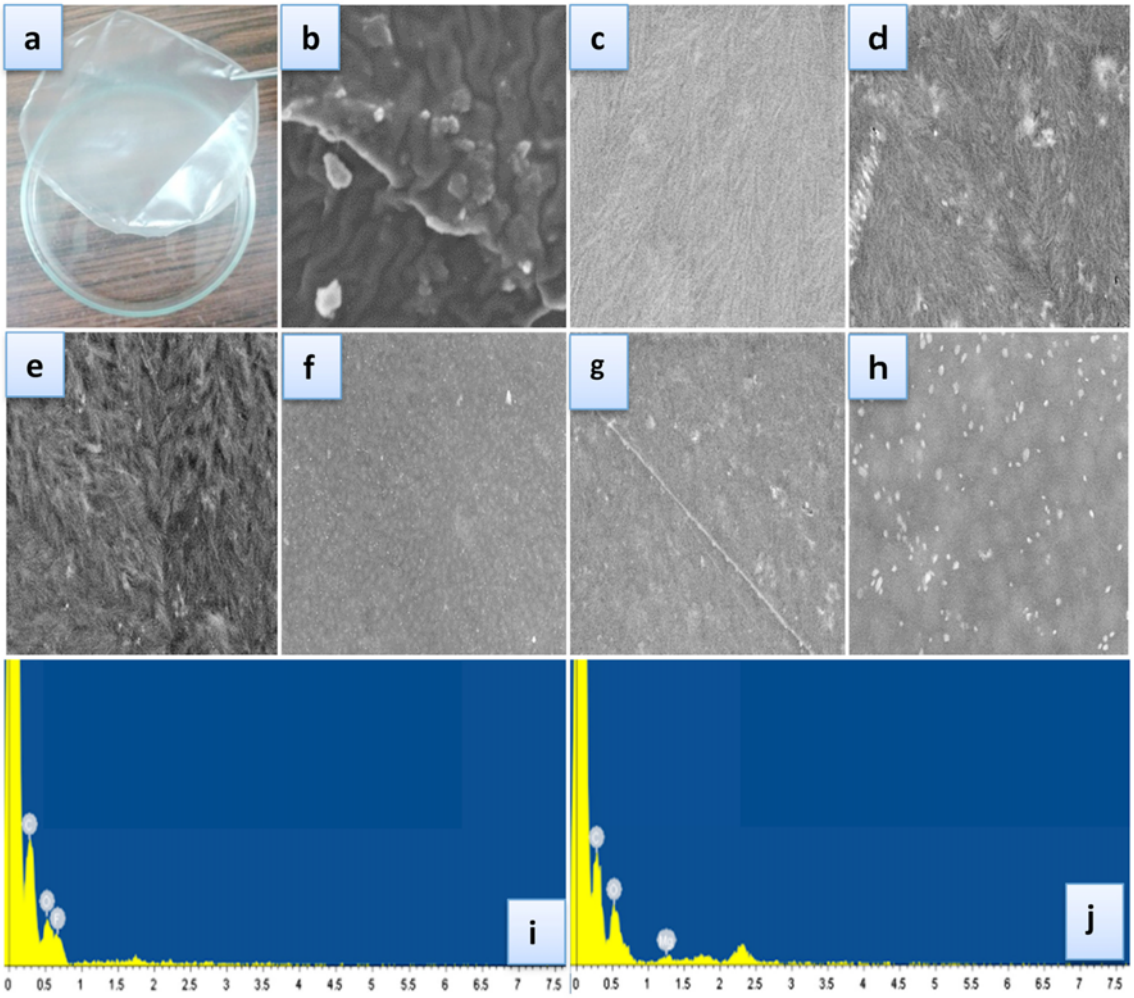

Figure 2. (a) Photograph of as-prepared thin film electrolyte**,** (b-g) SEM images of PEO-PVDF (b) polymer blend with varying salt concentrations (c) 3 wt% (d) 6 wt% (e) 9 wt% (f) 12 wt% (g) 15 wt% and (h) 18 wt% (i, j) EDAX profile of 15 and 18 wt% of salt concentrations.

in the number of mobile charge carriers in the polymer electrolytes. The derived room temperature conductivity data in the case of all the solid polymer-blend electrolytes are presented in Table I.

As seen in the complex impedance spectra (Figure 3(a)), the bulk resistance (R_b) decreases as a function of salt concentration raises up to 15 wt% followed by an apparent increase in R_b in the case of higher loading of salt content (18 wt%). It is obvious that the number of charge carrier increases as the salt concentration increases and results in the lowest R_b value for the particular concentration of 15 wt% salt and would exhibit a maximum conductivity of 1.2×10^{-5} S cm^{-1} at room temperature. In general, the conductivity mechanism of polymer electrolytes involved both the segmental motion of polymer chain and ion mobility. In particular, the charge carriers are produced by dissolving an appropriate salt in a polymer solution. Therefore, the degree of dissociation plays a crucial role to influence on the conductivity as a result of dissociated ions. However, the maximum conductivity of the PEO-PVDF blend electrolyte is reached when the Mg salt concentration is 15 wt% and then begins to drop beyond that concentration. The observed enhancement of ion transport in the blend electrolyte system may be attributed to the strong coordination of donor group of PEO and highly electro-negative F of PVDF with Mg ions that produces more number of dissociated ions wherein the polymer-blend already facilitates the segmental motion. An increasing trend of conductivity as the salt content is raised (Figure 3(c)) may be described as that at low salt content, a dilution effect is predominant whereas an average interionic distance decreases at higher loading of salt thus enhancing the ion associations.

Figure 3(d) depicts the behaviour of conductivity as a function of frequency for the six different compositions of the blended solid polymer electrolytes (PEO/PVDF-Mg[$(CF_3SO_2)_2N)_2$] where x=3, 6, 9, 12, 15, and 18 wt%, respectively, at room temperature (298 K) in the frequency domain 20 Hz - 1 MHz. It is obvious that the observed spectra establish the three distinct regions, *viz*., low frequency dispersive region relative

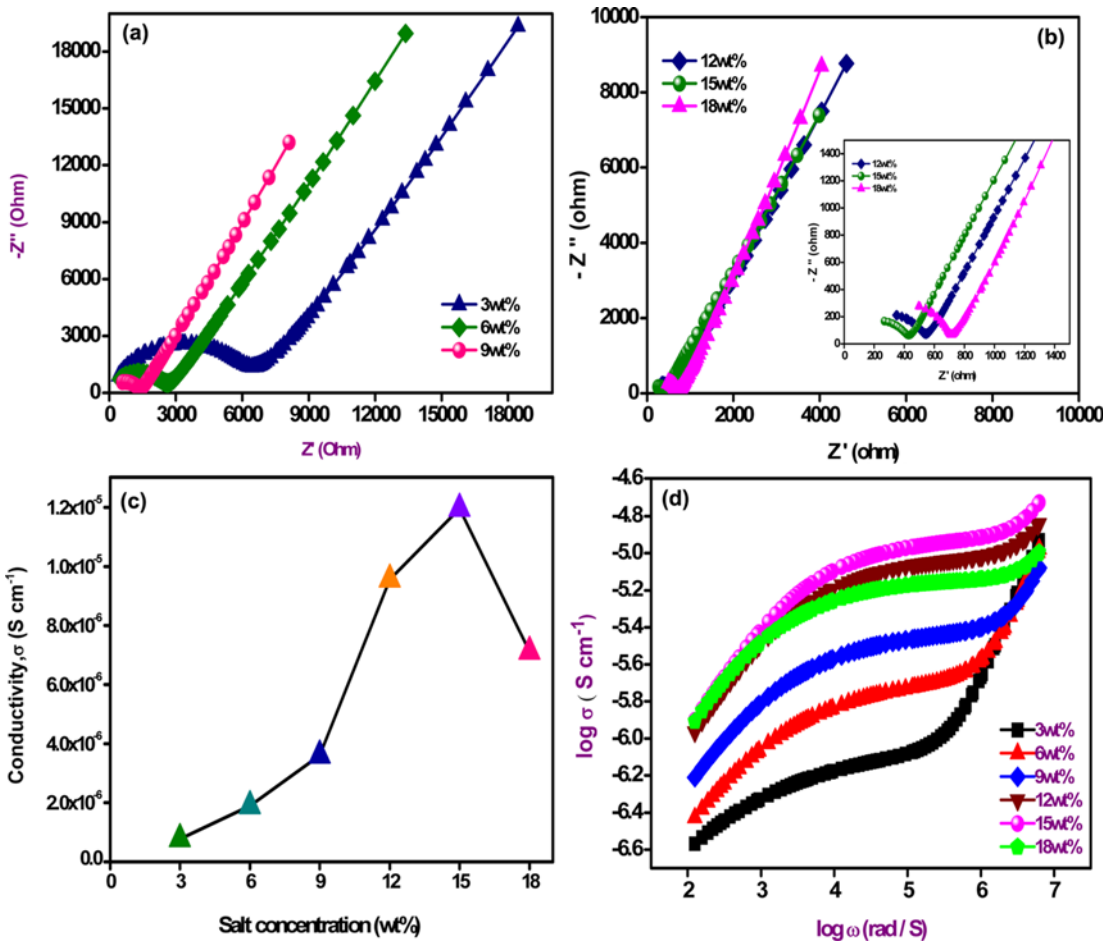

Figure 3. The complex impedance diagrams obtained at room temperature for the polymer-blend (PEO/PVDF) with different concentrations (a) 3, 6, and 9, (b) 12, 15, and 18 wt% of salt (insert shows the magnified view). (c) Variation of ionic conductivity as a function of salt concentration at room temperature. (d) Frequency dependent conductance spectra of polymer-blend electrolytes at room temperature.

Table I. Conductivity Values Obtained from Impedance Plot for Different Concentrations of Salt (x=3, 6, 9, 12, 15, and 18 wt%) at Room Temperature

PEO/PVDF-Mg[$(CF_3SO_2)_2N_2$)]	Conductivity (σ) S cm^{-1} at Room Temperature (298 K)
90:10+3 wt% salt	7.8×10^{-7}
90:10+6 wt% salt	1.9×10^{-6}
90:10+9 wt% salt	3.6×10^{-6}
90:10+12 wt% salt	9.5×10^{-6}
90:10+15 wt% salt	1.2×10^{-5}
90:10+18 wt% salt	7.1×10^{-6}

to the electrode polarization, a mid frequency plateau identical to the dc conductivity, and the high frequency dispersion region which could infer the frequency-dependent ion transport in good agreement with the well-known Jonscher's universal power law given by the relation.[27]

$$\sigma(\omega) = \sigma_o + A\omega^s \quad (2)$$

where $\sigma_o(\omega)$ is the dc conductivity, A the temperature-dependent pre-exponential factor and S is the fractional exponent value lying between 0 and 1. From the frequency response of conductivity spectrum (Figure 3(d)) each profile of the blended electrolyte system showed the dispersion in conductivity at the low frequency domain arising from the space-charge polarization at the electrode-electrolyte interface followed by the frequency-independent plateau which would correspond to the dc conductivity (σ_{dc}) of the samples. The fact that a sharp increase in conductivity is observed at higher frequency region may be attributed to the faster displacement of ions under the AC field.

Frequency Response of Electric Modulus Analysis. The frequency response of electrical modulus representation has been established and studied extensively to identify the electrical relaxation and the electrode polarization effect given by the relation.

$$M^* = I/\varepsilon^* = j\omega C_0 Z^* = M' + jM'' \quad (3)$$

where the angular frequency $\omega=2\pi f$ and C_0 is the vacuum capacitance of the electrochemical cell. M' and M'' denote the real and imaginary parts of modulus M^*, respectively.

A true electrical relaxation for the blended electrolytes with various salt concentration is usually identified by plotting the real (M') and imaginary (M'') part of electric modulus as a function frequency as presented in Figure 4(a) and (b). An almost zero value of M' at low frequency indicates the negligible contribution of the electrode polarization whereas a considerable raise in M' value as well as a shift in curves towards the high frequency region is observed as a function salt concentration increases up to 15 wt%. A similar trend has been observed in the imaginary part of the electrical modulus spectra for all the systems. A shift noticed in real and imaginary parts of electrical modulus and M'' values at high frequency region infers that the number of charge carrier increases at the interface as the salt concentration raise up to 15 wt%. The variation of real (M') and imaginary (M'') parts of electric modulus plots (Figure 4(a) and (b)) approaches zero at low frequency indicating that the electrode polarization phenomena making an insignificant contribution to the real and imaginary part of electric modulus. M' exhibits the same trend as that of M''. Since the maximum of modulus spectra M'' is found to shift toward higher frequency with an increase of salt concentration which implies that the mobile ions may have a shorter relaxation time. The asymmetric nature of the modulus peaks may be associated with the non-Debye nature of the material with a distribution of relaxation times.[28,29]

Frequency Response of Dielectric Spectra Analysis. The variation of dielectric constant real (ε') and dielectric loss imaginary (ε'') as a function of frequency for the six different blended polymer electrolytes is given in Figure 5(a) and (b). A steady increase in dielectric constant ε' is observed at low frequencies in the range of the salt concentration from 3 to 15 wt% and a slight decrease in ε' is noticed for the higher loading of salt (18 wt%) and gets into an abruptly constant value of ε' in the high frequency region for all the systems. A similar trend has also been observed in dielectric loss, ε''

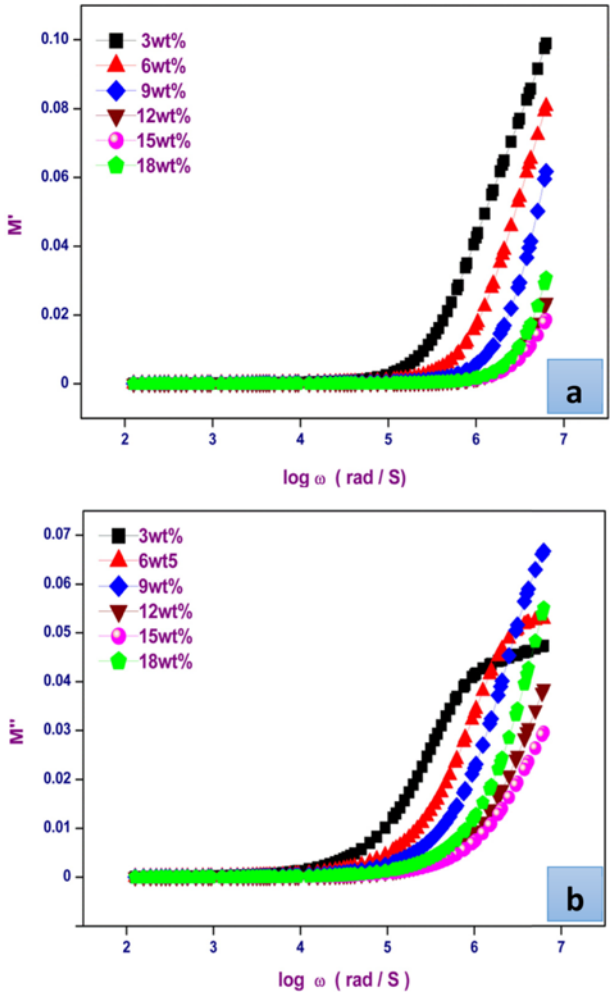

Figure 4. Frequency response of (a) real, M' and (b) imaginary, M'' parts of electric modulus obtained for all the as-prepared samples at room temperature.

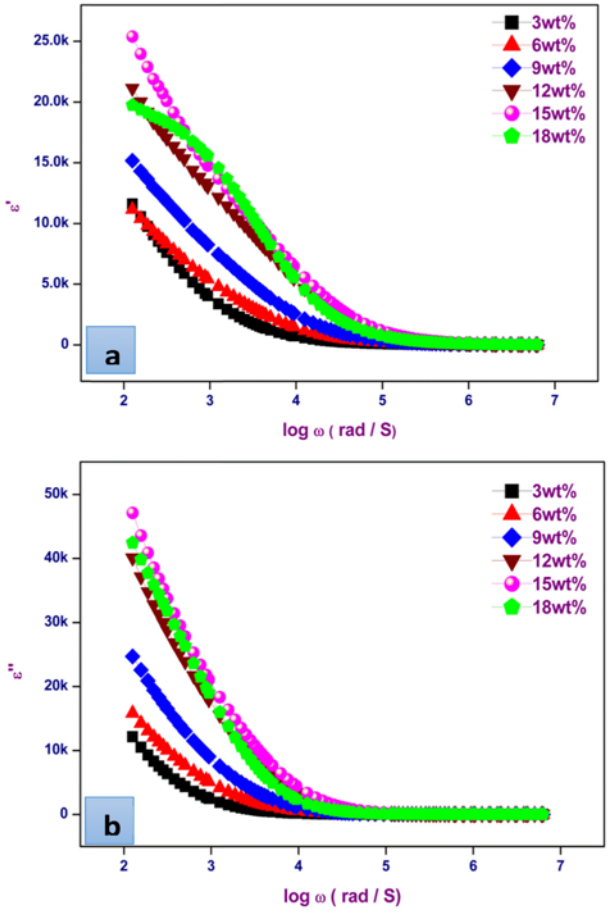

Figure 5. Frequency response of (a) real, ε' and (b) imaginary, ε'' parts of dielectric constant obtained for PEO-PVDF blend with six different salt concentrations at room temperature.

spectra as well at room temperature. The correlation of dielectric constant and loss profiles as a function of frequency has been analysed to identify the localized dielectric relaxation for all the six different salt concentration-added blend electrolytes at room temperature by using the given dielectric formalism, ε^*.

$$\varepsilon^* = \varepsilon' - j\varepsilon'' \quad (4)$$

where ε' is the real part and ε'' is the imaginary part of the dielectric constant. As seen in Figure 5(a) and (b), there is no relaxation peak observed up to 15 wt% salt and it begins to show as the small peak in the low frequency region in the case of 18 wt% salt added to the system. It is clearly evident that no polymer reorientation or cross-linking of polymers occurs until the loaded content of 15 wt% salt. It is apparent that the enhancement of both ε' and ε'' at low frequency may be ascribed as mainly due to the fact that the ions are allowed to accumulate freely and build up the charges near the electrode-electrolyte interface whereas the fact that both the values of ε' and ε'' decrease rapidly and reach nearly zero at higher frequency may be ascribed to the occurrence of a fast periodic reversal of the applied field and no time to orient themselves which limits the ion diffusion in the direction of the applied field.[27-30]

Conclusions

The impact of addition of magnesium bis (trifluoromethane sulfonimide) Mg [$(CF_3SO_2)_2N_2$)] salt on the electrical conductivity and transport characteristics within the polymer blend of PEO-PVDF has been investigated. The maximum electrical conductivity value on the order of 1.2×10^{-5} Scm^{-1} at room temperature (298 K) was registered for the typical sample containing 15 wt% salt. The XRD data revealed the occurrence of a considerable decrease in the degree of crystallinity and the structural modification was found to be in good agreement with the electrical conductivity data. Detailed surface morphological features have also been examined through SEM analysis. An in-depth frequency response analysis of electric modulus and dielectric properties has revealed that the blended electrolyte complex shows the feasibility of polymer flexibility with no conductivity relaxation. Further analysis needs to be performed in order to identify the reversibility of magnesium deposition and dissolution processes.

Acknowledgments. The authors wish to thank University of Madras for the financial support received for this work in the form of a research project. One of the authors (RR) greatly acknowledges University of Madras for the award of University Research Fellowship (URF).

References

(1) M. Armand and J. M. Tarascon, *Nature,* **451**, 652 (2008).
(2) J. M. Tarascon and M. Armand, *Nature*, **414**, 359 (2001).
(3) W. H. Meyer, *Adv. Mater.*, **10**, 439 (1998).
(4) O. Chusid, Y. Gofer, H. Gizbar, Y. Vestfrid, and E. Levi, *Adv. Mater.,* **15**, 627 (2003).
(5) S. Jeremias, G. A. Giffin, A. Moretti, and S. Jeong, *J. Phys. Chem. C*, **118**, 28361 (2014).
(6) H. S. Kim, T. S. Arthur, G. D. Allred, and J. Zajicek, *Nat. Commun*., **2**, 427 (2011).
(7) D. Aurbach, A. Schechter, O. Chusid, and H. Gizbar, *J. Power Sources*, **28**, 97 (2001).
(8) A. Magistris and K. Singh, *Polym. Int.*, 28277 (1992).
(9) J. Xia, X. Qiua, J. Lib, Tang, and W. Zhu, *J. Power Sources,* **157**, 501 (2006).
(10) G. G. Kumar and N. Munichandraiah, *J. Power Sources*, **102**, 46 (2001).
(11) G. P. Pandey and S. A. Hashmi, *J. Power Sources,* **187**, 627 (2009).
(12) A. R. Polu, R. Kumar, and K. V. Kumar, *Adv. Mater. Lett.,* **3**, 406 (2012).
(13) G. G. Kumar and N. Munichandraiah, *Electrochim. Acta,* **44**, 2663 (2001).
(14) G. G. Kumar, and N. Munichandraiah, *Electrochim. Acta,* **47**, 1013 (2002).
(15) M. Morita, N. Yoshimoto, and S. Yakushiji, *Electrochem. Solid-State Lett.,* **4**, A177 (2001).
(16) H. D.Yoo, I. Shterenberg, and Y. Gofer, *Energy Environ. Sci.,* **6**, 2265 (2013).
(17) R. Mohtadi and F. Mizuno, *Beilstein J. Nanotechnol*., **5**, 1291 (2014).
(18) C. Liebenowa, *Electrochim. Acta,* **43**, 1253 (1998).
(19) D. Aurbach, Z. Lu, A. Schechter, and Y. Gofer, *Nature*, **407**, 724 (2000).
(20) D. Aurbach, I. Weissman, and Y. Gofer, *Chem. Rec.*, **3**, 61 (2003).
(21) T. T. Tran, W. M. Lamanna, and M. N. Obrovac, *J. Electrochem. Soc.*, **159**, A2005 (2012).
(22) D. Aurbach, A. Schechter, and M. Moshkovich, *J. Electrochem. Soc.*, **148**, A1004 (2001).
(23) Y. Shaoa, N. N. Rajput, H. M. Hua, and T. Liu, *Nano Energy*, **12**, 750 (2015).
(24) N. Yoshimoto, S. Yakushiji, and M. Ishikawa, *Electrochim. Acta*, **48**, 2317 (2003).
(25) J. S. Oh, J. M. Ko, and D. W. Kim, *Electrochim. Acta*, **50**, 903 (2004).
(26) N. H. Zainol, Z. Osman, and L. Othman, *Adv. Mater. Res.,* **686**, 137 (2013).
(27) A. K. Jonscher, *Dielectric Relaxation in Solids*, Chelsea Dielectrics Press, London, 1983.
(28) S. A. Suthanthiraraj, R. Kumar, and B. J. Paul, *J. Solid State Electrochem.,* **15**, 561 (2011).
(29) V. D. Noto, M. Vittadello, and S. Lavina, *J. Phys. Chem. B,* **105**, 4584 (2001).
(30) M. Piccolo, G. A. Giffin, and K. Vezzu, *ChemSusChem*, **6**, 2157 (2013).